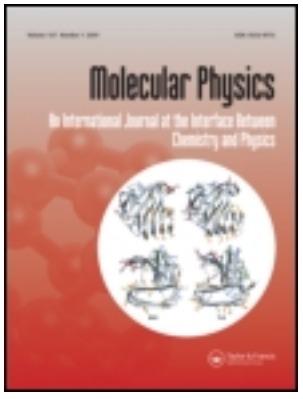

Molecular Physics: An International Journal at the Interface Between Chemistry and Physics
Publication details, including instructions for authors and subscription information:
http://www.tandfonline.com/loi/tmph20

Monte Carlo simulations of intrinsic anchoring in nematic liquid crystals based on spatially anisotropic pair potential

Y. Zhang [a b c] & Z. Zhang [c]

[a] Changchun Institute of Optics, Fine Mechanics and Physics, Chinese Academy of Sciences, Changchun, China

[b] Graduate School of the Chinese Academy of Sciences, Beijing, China

[c] Hebei University of Technology, Tianjin, China

Version of record first published: 21 Feb 2007

To cite this article: Y. Zhang & Z. Zhang (2007): Monte Carlo simulations of intrinsic anchoring in nematic liquid crystals based on spatially anisotropic pair potential, Molecular Physics: An International Journal at the Interface Between Chemistry and Physics, 105:1, 85-94

To link to this article: http://dx.doi.org/10.1080/00268970601132005

Molecular Physics, Vol. 105, No. 1, 10 January 2007, 85–94

Monte Carlo simulations of intrinsic anchoring in nematic liquid crystals based on spatially anisotropic pair potential

Y. ZHANG*†‡§ and Z. ZHANG§

†Changchun Institute of Optics, Fine Mechanics and Physics,
Chinese Academy of Sciences, Changchun, China
‡Graduate School of the Chinese Academy of Sciences, Beijing, China
§Hebei University of Technology, Tianjin, China

(*Received 16 September 2006; in final form 10 November 2006*)

The free surfaces of nematic liquid crystals are studied based upon the molecular pair potential model, which is spatially anisotropic and dependent on elastic constants of liquid crystals. The study is based on the simple cubic lattice model with the aid of Monte Carlo simulation. An elastic deformation is imposed, forming a hybrid cell-like nematic sample so that the anchoring at free nematic interfaces (intrinsic anchoring) is well studied. It is found that the preferred orientation at the free interface and the corresponding extrapolation length change with the modification of potential parameters, but are not dependent on temperature.

1. Introduction

Based upon anisotropic dispersive forces, Maier and Saupe [1, 2] constructed a molecular field theory for nematic liquid crystals. Lebwohl and Lasher [3] made a Monte Carlo simulation study of the model system consisting of cylindrically symmetric particles confined to the sites of a simple cubic lattice, using the Lebwohl–Lasher pair potential (also called L–L pair potential). However, this L–L potential only describes spatially isotropic interaction and does not depend on the relative position of the particles. In 1996, Gruhn and Hess proposed a spatially anisotropic pair potential depending on the relative position of the particles [4]. It approximately reproduces the elastic free energy density, so that the parameters defining the pair potential can be expressed in terms of the elastic constants. With that, a Monte Carlo simulation on PAA in homogeneous nematic phase was made by Romano [5]. In addition, Romano has dealt with the above potential model on 2-demensional lattices using Mean Field Theory and Monte Carlo simulations [6].

Liquid crystals in restricted geometries are of great interest [7]. In confined nematic liquid crystals with a large surface-to-volume ratio, the aligning effects of the confining surfaces are crucial in determining the equilibrium director configuration. Two major contributions determine the equilibrium director configuration. One is the nematic–substrate interactions and the other is the incomplete anisotropic nematic–nematic interactions in the vicinity of the sample surface. The former is external anchoring and the later is intrinsic anchoring (the anchoring at free nematic interfaces) [8]. The study of anchoring at free nematic interfaces is of importance both in its own right and as a reference for fully confined systems. One of the first experimental investigations of free nematic liquid crystal (NLC) surfaces observed the surface alignment using a light reflection technique and found that p-azoxyanisole (PAA) favours planar ordering [9]. Subsequent work [10] confirmed this result for PAA. Later, another experiment considered the intrinsic anchoring strength and showed that the corresponding extrapolation length is above 100 nm [11]. It is worth stressing that molecular theories are able to model the free interfacial behaviors. A number of simulations of the free interface of nematic liquid crystals have been performed by different potential models so as to investigate how the experimental interfacial phenomena are related to the molecular potentials. For example, intrinsic anchoring has been analysed by means of a pseudo-molecular model which uses the Maier–Saupe approximation for intermolecular interaction [12]. In addition, some other studies concentrated on the Gay–Berne potential [13] model but chose different parameters [14–16].

*Corresponding author. Email: zyj513@hebut.edu.cn

Molecular Physics
ISSN 0026–8976 print/ISSN 1362–3028 online © 2007 Taylor & Francis
http://www.tandf.co.uk/journals
DOI: 10.1080/00268970601132005

In this paper, we present a Monte Carlo study of the free nematic interfacial behaviour based on the Gruhn–Hess pair potential. We estimate the change of the corresponding extrapolation length with the pair potential parameters and the temperature. And we also study the preferred orientation (the easy axis) at free nematic interfaces. Furthermore, we compare our results with some experiments and references.

2. Simulation models

Consider a nematic crystal (NLC) lattice model. From [4], the nearest-neighbour pair potential takes the form

$$U_{ik} = \varepsilon\left\{\lambda[P_2(a_i) + P_2(a_k)] + \mu\left(a_i a_k b_{ik} - \frac{1}{9}\right) + \nu P_2(b_{ik}) + \rho[P_2(a_i) + P_2(a_k)]P_2(b_{ik})\right\} \quad (1)$$

$$\boldsymbol{r} = \boldsymbol{p_i} - \boldsymbol{p_k}, \quad \boldsymbol{s} = \frac{\boldsymbol{r}}{|\boldsymbol{r}|}, \quad a_i = \boldsymbol{u_i}\cdot\boldsymbol{s}, \quad a_k = \boldsymbol{u_k}\cdot\boldsymbol{s}, \quad b_{ik} = \boldsymbol{u_i}\cdot\boldsymbol{u_k} \quad (2)$$

ε denotes a positive quantity setting scaled temperature, i.e. $T^* = k_B T/\varepsilon$. Here P_2 is the second-order Legendre polynomial; $\boldsymbol{p_i}$ and $\boldsymbol{p_k}$ are three-component dimensionless lattice-point coordinates; $\boldsymbol{u_i}$ and $\boldsymbol{u_k}$ denote three-component unit vectors describing the orientations of the two particles; $\boldsymbol{s}$ is a unit vector pointing from the centre of mass of molecule i to the centre of mass of molecule k.

The potential parameters are related to the elastic constants K_i ($i = 1, 2, 3$) as follows [5]

$$\lambda = \frac{1}{3}\Lambda(2K_1 - 3K_2 + K_3) \quad (3a)$$

$$\mu = 3\Lambda(K_2 - K_1) \quad (3b)$$

$$\nu = \frac{1}{3}\Lambda(K_1 - 3K_2 - K_3) \quad (3c)$$

$$\rho = \frac{1}{3}\Lambda(K_1 - K_3) \quad (3d)$$

where the factor Λ is defined by setting $\nu = -1$. When $\lambda = \mu = \rho = 0$ and $\nu = -1$, the pair potential reduces to the L–L model. The pair potential given by equation (3) is called model I (M I). When dealing with Fréedericksz transition by supposing perfect nematic order in a slab, we can obtain equations (3b) (3c) (3d) but cannot find a relation between λ and K_i (see Appendix 2). However, under three-dimensional period boundary conditions, upon summing over all interacting pairs, the terms $\lambda[P_2((a_i)) + P_2(a_k)]$ in the pair potentials cancel out identically [17], i.e. the value of λ does not influence the description of the NLC bulk properties. So our result, in fact, is consistent with M I in three-dimensional periodic boundary conditions [18]. In addition, as seen from Appendix 3, M I does not induce intrinsic anchoring at free interfaces in perfect nematic order, which is therefore not suitable for studies of intrinsic anchoring. Therefore, we cannot neglect λ when considering the behaviour of interfaces. We expect a modification of λ for M I to describe the behaviour of nematic interfaces, i.e. $\lambda + c$ instead of λ. Intrinsic anchoring is planar when $c > 0$, and homeotropic when $c < 0$. When c is zero, it is M I. By doing this, the bulk properties being described do not change.

There is another mapping scheme from the elastic free energy density to the potential parameters (called model II, i.e. M II) [19]. By M II, we can estimate the preferred orientation at the free interface, i.e. intrinsic anchoring is planar when $K_1 < K_3$ and homeotropic when $K_1 > K_3$. So we also consider its results from intrinsic anchoring [20] (see Appendix 3).

Anchoring effects usually are characterized within phenomenological approaches by two parameters: the easy axis and the anchoring strength W. They can also be described by the extrapolation length $b = K/W$ (K denoting the Frank elastic constant). In our discussion, we define the extrapolation length $b = K_1/W$. Here K_1 is the splay elastic constant. An elastic distortion is imposed to measure the anchoring strength. The nematic–substrate interaction [21] is given by

$$U_S = -\varepsilon_S P_2(\boldsymbol{u}_i \cdot \boldsymbol{e}). \quad (4)$$

Here, $\boldsymbol{e}$ is the easy axis of the substrate and $\boldsymbol{u}_i$ is a unit vector along the symmetry axis of the molecule i which is in the nearest layer from the substrate. We define a dimensionless anchoring strength parameter as $w = \varepsilon_s/\varepsilon$.

For MII, as shown in Appendix 3, intrinsic anchoring is planar when $K_1 < K_3$ and homeotropic when $K_1 > K_3$. Experimental investigations of free nematic surfaces find that PAA ($K_1 < K_3$) favours planar ordering [9]. Accordingly, we try to choose two liquid crystal materials to make the numerical calculation. One is PAA at 120°C [22]. The elastic constants are

$$K_1 = 7.0 \times 10^{-12}\,\mathrm{N}, \quad K_2 = 4.3 \times 10^{-12}\,\mathrm{N}, \quad K_3 = 17.0 \times 10^{-12}\,\mathrm{N} \quad (5)$$

which satisfy $K_1 < K_3$. Setting $\nu = -1$, the pair potential parameters are

$$\lambda = 0.79039, \quad \mu = -1.0611, \quad \nu = -1, \quad \rho = -0.43668 \quad (6)$$

Following [23], we choose a second liquid crystal material which satisfies $K_1 > K_3$. The elastic constants are

$$K_1 = 5.43 \times 10^{-12}\,\mathrm{N}, \quad K_2 = 2.51 \times 10^{-12}\,\mathrm{N}, \quad K_3 = 4.07 \times 10^{-12}\,\mathrm{N}. \tag{7}$$

We call this 'X' below. In the same way, the pair potential parameters are

$$\lambda = 1.19935, \quad \mu = -4.25932, \quad v = -1, \quad \rho = 0.22042. \tag{8}$$

We choose two NLC slabs in order to study the intrinsic anchoring easy axis and the intrinsic anchoring strength, as shown in figure 1(a) and (b). In figure 1(a), the top ($z = d$) interface is taken to be a substrate with strong external anchoring ($w = 1$) and the easy axis $\boldsymbol{e} = (0,0,1)$. The bottom ($z = 0$) interface where the intrinsic anchoring will be measured is a free interface denoted by a dashed line. Figure 1(b) shows that the top ($z = d$) interface is taken to be a substrate with strong external anchoring ($w = 1$) and easy axis $\boldsymbol{e} = (1,0,0)$. The bottom ($z = 0$) interface is also a free interface. We simulate using the first slab (figure 1(a)) when the easy axis of the free interface is planar and using the second slab (figure 1(b)) when the easy axis of the free interface is homeotropic, so that the two slabs can form hybrid cell-like nematic samples.

3. Simulation aspects

Simulations have been performed on cubic samples with a simulation box size 32^3. We have used periodic conditions in the x and y directions, and considered interactions only between nearest neighbours. For the numerical calculations, the scaled temperature $T^*(T^* = k_B T/\varepsilon)$ is introduced. We apply the Metropolis algorithm [24] to update the lattice and to find the state of the lowest energy. Instead of comparing different configurations, one (arbitrary) director distribution is taken and the free energy E_p is calculated. Then we select a random point of the configuration and calculate the energy E_n, altered by a random amount and the energy difference between old and new configuration, ΔE, is calculated. If ΔE is negative, i.e. the altered director field has a lower energy than the unaltered one, the move is accepted. If ΔE is positive, i.e. the change of director increases the energy, the move is not immediately discarded but accepted with a probability of $p = e^{-\Delta E/k_B^T}$. This procedure is inspired by the way a real liquid crystal reaches its thermal equilibrium. Our equilibration runs take 10^5 cycles and production runs take 10^5 cycles.

We need to calculate the director profile $\theta(z)$ in order to measure the extrapolation length. So we calculated the second rank tensor after its reaching thermal equilibrium.

$$Q_{\alpha\beta}(z) = \frac{\left(3\left\langle u_i^\alpha u_i^\beta \right\rangle_z - \delta_{\alpha\beta}\right)}{2}. \tag{9}$$

Here, α and β can be x, y or z, and u_i^α refers to the α component of the unit vector $\boldsymbol{u}_i$. First, the average $\langle \ldots \rangle_z$ is performed over all particles for the current configuration in the layer centred at z. Then the current second rank ordering tensor is diagonalized. Accordingly, the director is identified by the eigenvector associated with the eigenvalue possessing the largest magnitude, and the second-order parameter is equal to the largest magnitude eigenvalue. Lastly, the director and the second-order parameter are averaged over the production Monte Carlo cycles.

4. Results and discussion

We have studied the intrinsic anchoring by setting different low modification values. We can see from the

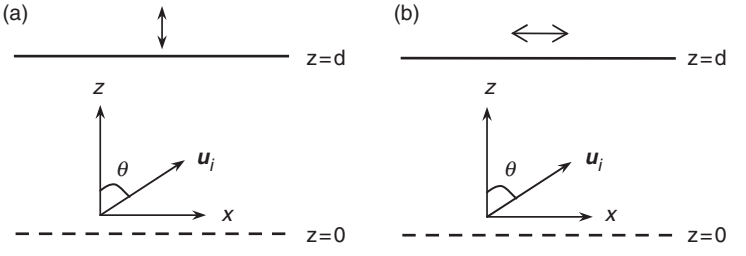

Figure 1. Two NLC slabs (a) the top interface is a substrate with strong external hometropic anchoring and the bottom interface is a free interface described with a dashed line. (b) the top interface is a substrate with strong external planar anchoring and the bottom interface is a free interface. $\theta = \theta(z)$ is the usual polar angle which is measured with respect to the z-axis.

simulation results that there is no twist distortion (except the simulation error of $\leq 5^\circ$). On the other hand, the anchoring at the free interface is homeotropic when $c > 0$ and planar when $c < 0$. This is consistent with our prediction in perfect nematic order (see Appendix 3). By M II, we have shown the experimental result that the free interface for PAA favours planer alignment. In addition, we also note the other result, which is still not identified by experiments, i.e. the intrinsic anchoring easy axis is homeotropic when $K_1 > K_3$. In order to obtain the results according to M II, we choose $c = -0.4$, -0.2, 0.0 for PAA and $c = 0.0$, 0.1, 0.3 for X, which forms two kinds of hybrid boundary conditions. For the hybrid boundary conditions in figure 1(a), the Frank elastic theory gives the equation of the bottom surface ($z = 0$)

$$\left(1 + \frac{K_3}{K_1}\cot^2\theta(0)\right)\left(\frac{d\theta}{dz}\right)_0 = \left(\frac{W}{K_1}\right)_0 \cot\theta(0) \qquad (10)$$

and we can obtain the equation of the bottom surface ($z = 0$, figure 1(b))

$$\left(1 + \frac{K_3}{K_1}\cot^2\theta(0)\right)\left(\frac{d\theta}{dz}\right)_0 = -\left(\frac{W}{K_1}\right)_0 \cot\theta(0). \qquad (11)$$

According to equations (10) and (11), we can determine $(K_1/W)_0$ simply by the director polar angle profile $\theta(z)$ and $(d\theta/dz)_0$. We note that the nematic order parameter is not a constant near sample boundaries in several molecular layers. So the extrapolation of the profile towards the surface must be calculated from far enough in the bulk where the order parameter is a constant (the order parameter difference between nearest layers $\Delta Q \leq 0.1$). Certainly, we also note that whenever $(K_1/W)_0$ approaches d (for weak anchoring or in a thin sample), $(d\theta/dz)_0$ and consequently $(K_{11}/W)_0$ are accompanied by a significant systematic error.

As seen from the simulation results for PAA (table 1, figure 2 and figure 3), the intrinsic anchoring favours planer alignment. And the corresponding intrinsic extrapolation length b is independent of the scaled temperature, which is identical with the result in [8]. Moreover, b depends on the modification c, although the bulk transition temperature ($T^*_{NI} = 1.368 \pm 0.002$ [5]) shows no dependence on it. As seen in table 1, when $c = -0.2$, $b = (10.0 \pm 0.1)a$; when $c = -0.4$, $b = (4.6 \pm 0.1)a$. It increases with increasing c. The experiment shows that the intrinsic anchoring strength is so weak that the corresponding extrapolation length is above 100 nm [11]. Thus, we can obtain quantitative agreement between our results and experiments by modulating the value of c. Certainly, we also note that b is very different when the

Table 1. Extrapolation length b in units of lattice spacing a for PAA and X at different modifications c.

	c	$b(a)$
PAA($T^*_{NI} = 1.368 \pm 0.002$)	-0.2	10.0 ± 0.1
$T^* \leq 1.30$	-0.4	4.6 ± 0.1
X($T^*_{NI} = 2.148 \pm 0.002$)	0.1	13.9 ± 0.05
$T^* \leq 2.06$	0.3	3.5 ± 0.06

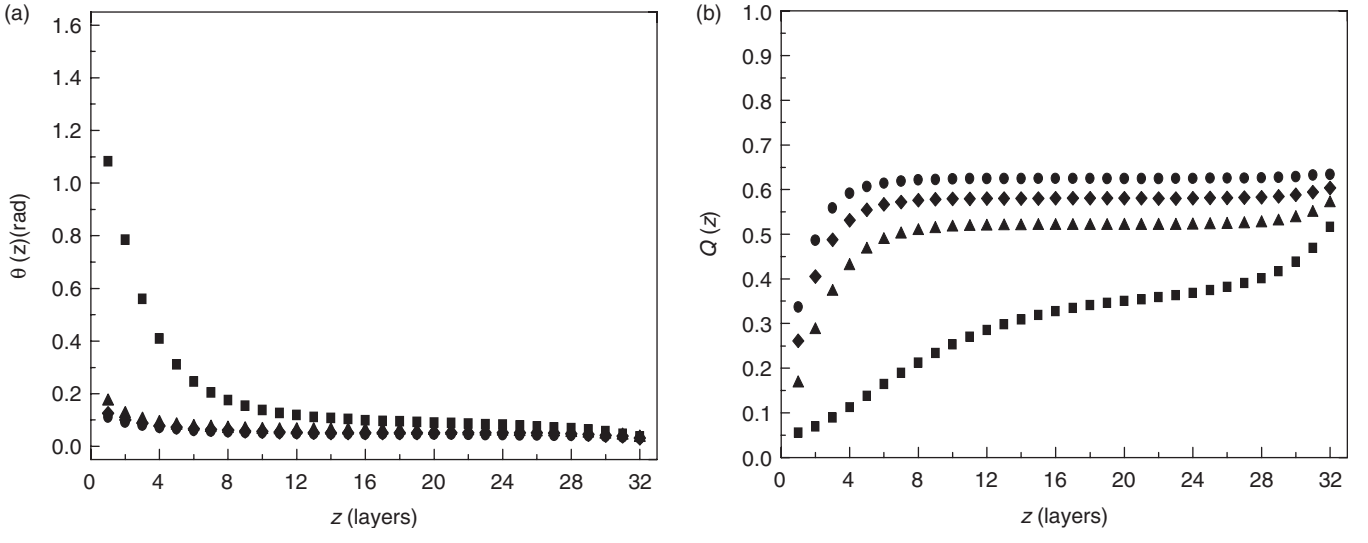

Figure 2. NLC slab with homeotropic anchoring at $z = 0$ and $c = -0.4$ for PAA. The scaled temperature: $T^* = 1.20$, $T^* = 1.25$, $T^* = 1.30$ and $T^* = 1.36$ (circles, diamonds, triangles, and squares, respectively); (a) director; (b) order parameter.

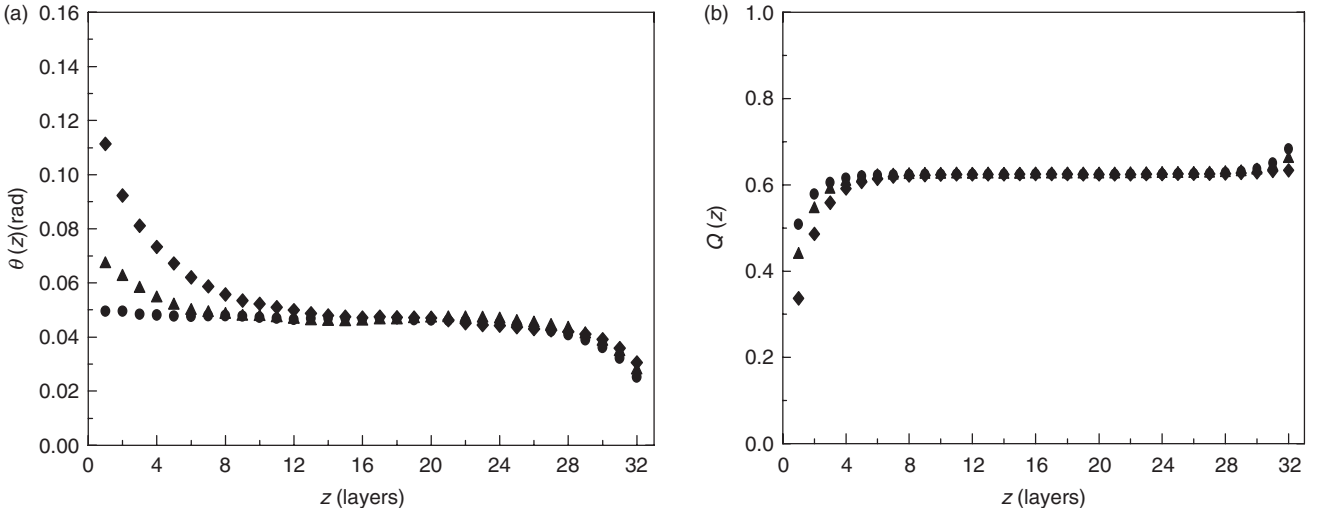

Figure 3. NLC slab with homeotropic anchoring at $z=0$ and $T^*=1.20$ for PAA. The value of modification: $c=0$, $c=-0.2$ and $c=-0.4$ (circles, triangles, and diamonds, respectively); (a) director; (b) order parameter.

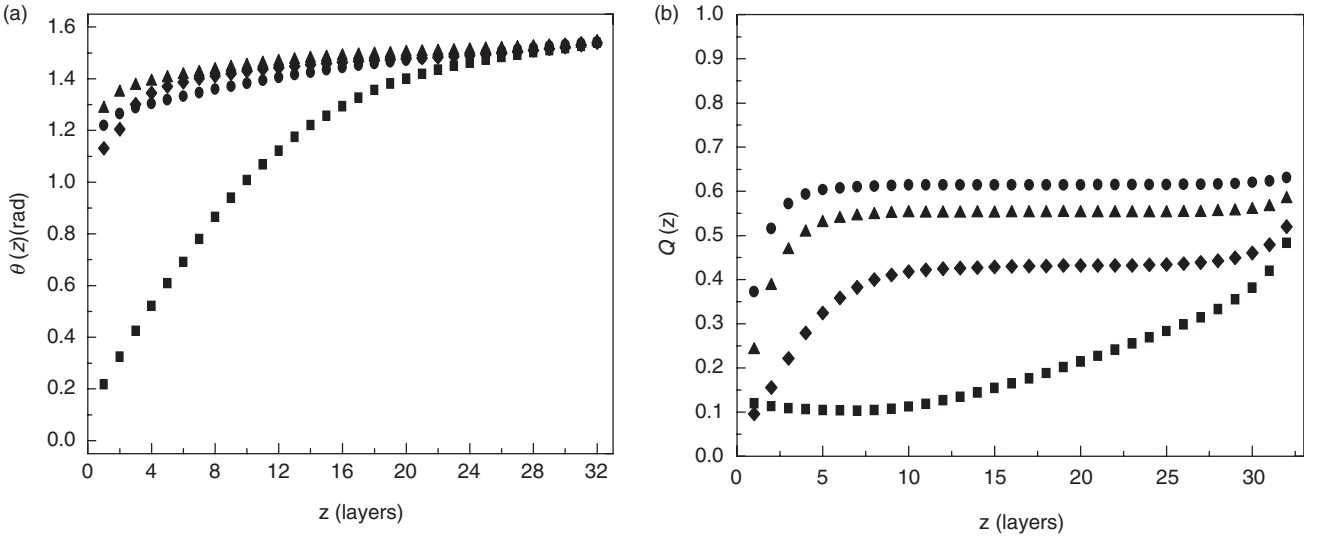

Figure 4. NLC slab with planar anchoring at $z=0$ and $c=0.1$ for X. The scaled temperature: $T^*=1.90$, $T^*=2.00$, $T^*=2.10$ and $T^*=2.14$ (circles, diamonds, triangles, squares, respectively); (a) director; (b) order parameter.

nematic-isotropic (NI) transition temperature is approached, since the layers near surfaces have reach the isotropic phase.

For X (table 1, figures 4 and 5), the intrinsic anchoring is homeotropic. And the intrinsic extrapolation length b increases with modification c decreasing and is independent of temperature. For X, when $c=0.1$, $b=(13.9\pm0.05)a$; when $c=0.3$, $b=(3.5\pm0.06)a$. We also simulate the transition temperature in the bulk sample for X to be $T^*_{NI}=k_BT_{NI}/\varepsilon=2.148\pm0.002$. When the NI transition temperature is approached, b is also different.

Certainly, we also note that both PAA and X cannot favour any orienting effects at the free interface when $c=0$. That is, M Ī cannot produce any orienting effects at a free nematic surface. This is consistent with the description in perfect nematic order [20] (see Appendix 3).

Therefore, for different liquid crystal materials, we can choose different modifications c, i.e. different models to describe their properties. By doing this, we can obtain the corresponding results with experiments and predict undiscovered properties of nematic liquid crystals.

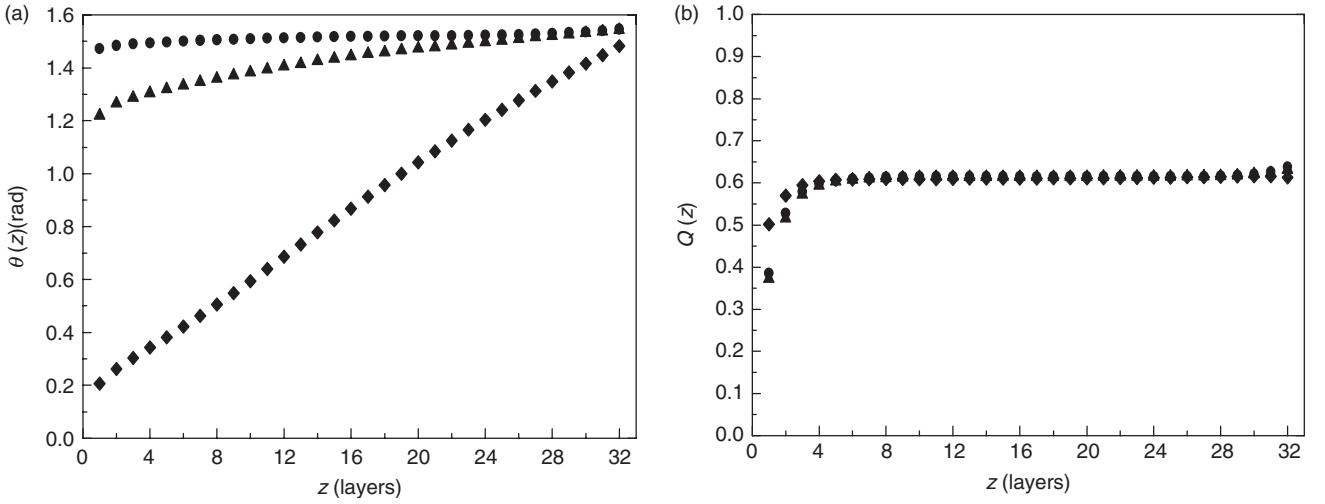

Figure 5. NLC slab with planar anchoring at $z=0$ and $T^*=1.90$ for X. The value of modification: $c=0$, $c=0.1$ and $c=0.3$ (circles, triangles, and diamonds, respectively); (a) director; (b) order parameter.

Acknowledgments

This work was supported by the Natural Science Foundation of Hebei Province, China (Grant No. 103002), and the Key Subject Construction Project of Hebei Provincial University.

Appendix

Study of distortions in NLC slabs based upon spatially anisotropic pair potential

Distortions of NLC slabs are studied based upon the spatially anisotropic pair potential model. The perfect nematic order is assumed in the theoretical treatment, which means the orientation of the molecular long axis coincides with the director of liquid crystal and the total free energy equals the total interaction energy. We investigate three kinds of the basic Fréedericksz transition and the director profiles at the free interfaces.

A.1. Fundamental equations

In order to compare with M I, we introduce M II for which the potential parameters related to the elastic constants K_i are as follows [19]

$$\lambda = \frac{2}{3}\Lambda(K_1 - K_2) \tag{A1a}$$

$$\mu = 3\Lambda(-K_1 + 2K_2 - K_3) \tag{A1b}$$

$$\nu = -\frac{2}{3}\Lambda K_2 \tag{A1c}$$

$$\rho = 0. \tag{A1d}$$

We study distortions of NLC slabs based upon M I and M II (i.e. equations (1), (2), (3) and (A1)). Our NLC slab is composed of n molecular layers (n is finite). The surfaces of the slab are assumed to be normal to the z axis so as to remove the homogeneity in the z direction but not in the $x-y$ plane. We label the molecular layers parallel to the surfaces by j, with $j=1$ and $j=n$ denoting the two surface layers. In the hypothesis of perfect nematic order, $\boldsymbol{u}_i$ coincides with the director of the liquid crystals (the statistical average of $\boldsymbol{u}_i$) and the total free energy coincides with the total intermolecular energy. Furthermore, we assume the molecular orientation changes only in the $x-z$ plane. The director $\boldsymbol{u}_i$ can be parameterized by the polar angle θ (the angle between the director and the layer normal)

$$\boldsymbol{u}_i = (\sin\theta_i, 0, \cos\theta_i). \tag{A2}$$

If the molecule i is in the jth layer, $\theta_i=\theta_j$. For the molecule i and its six neighbours, the unit vector $\boldsymbol{s}$ is given by

$$\boldsymbol{s}_{i1} = (-1,0,0), \quad \boldsymbol{s}_{i2} = (1,0,0), \quad \boldsymbol{s}_{i3} = (0,-1,0)$$
$$\boldsymbol{s}_{i4} = (0,1,0), \quad \boldsymbol{s}_{i5} = (0,0,-1), \quad \boldsymbol{s}_{i6} = (0,0,1). \tag{A3}$$

Substituting equations (A2) and (A3) into equations (1) and (2), we obtain the total energy per molecule in

the jth layer

$$U(j)=\sum_{k=1}^{6}U_{ik}=2\varepsilon\left\{(\lambda+\rho)\left(3\sin^2\theta_j-1\right)+\mu\left(\sin^2\theta_j-\frac{1}{9}\right)+\nu\right\}+2\left(-\frac{1}{9}\mu+\nu-\lambda-\rho\right)$$
$$+(1-\delta_{jn})\left\{\left[\lambda+\frac{3}{2}\rho\cos^2\left(\theta_j-\theta_{j+1}\right)-\frac{1}{2}\rho\right]\left[\frac{3}{2}\left(\cos^2\theta_j+\cos^2\theta_{j+1}\right)-1\right]+\mu\left[\cos\theta_j\cos\theta_{j+1}\cos\left(\theta_j-\theta_{j+1}\right)-\frac{1}{9}\right]\right.$$
$$\left.+\nu\left[\frac{3}{2}\cos^2\left(\theta_j-\theta_{j+1}\right)-\frac{1}{2}\right]\right\}+\left(1-\delta_{j1}\right)\left\{\left[\lambda+\frac{3}{2}\rho\cos^2\left(\theta_j-\theta_{j-1}\right)-\frac{1}{2}\rho\right]\left[\frac{3}{2}\left(\cos^2\theta_j+\cos^2\theta_{j-1}\right)-1\right]\right.$$
$$\left.+\mu\left[\cos\theta_j\cos\theta_{j-1}\cos\left(\theta_j-\theta_{j-1}\right)-\frac{1}{9}\right]+\nu\left[\frac{3}{2}\cos^2\left(\theta_j-\theta_{j-1}\right)-\frac{1}{2}\right]\right\}. \tag{A4}$$

Here we have introduced two factors $(1-\delta_{j1})$ and $(1-\delta_{jn})$, since molecules in the first layer have no lower neighbouring molecules and molecules in the nth layer have no upper neighbouring molecules.

If an external magnetic field $\boldsymbol{H}$ is applied to the NLC molecular, the potential of a NLC molecule induced by magnetic fields is [25]

$$f_m=-\frac{1}{2}\eta_a(\boldsymbol{H}\cdot\boldsymbol{u}_i)^2 \tag{A5}$$

where $\eta_a=\eta_{//}-\eta_\perp$ is the magnetic anisotropy of NLC molecule. If the molecule i is in the jth layer, equation (A5) gives

$$f_m(j)=-\frac{1}{2}\eta_\alpha(H_x\sin\theta_j+H_z\cos\theta_j)^2 \tag{A6}$$

The total energy of the sample (except the surface interaction energy) is obtained by summing up the single molecular energies given by equations (A4) and (A5) over all j layers

$$F=\sigma\sum_{j=1}^{n}\left[\frac{1}{2}U(j)+f_m(j)\right] \tag{A7}$$

where σ is the molecular density per unit surface.

The total free energy given by equation (A7) should be minimized with respect to all variables θ_j, leading to the necessary condition

$$\frac{\partial F}{\partial\theta_j}=0\quad(j=1,2,\ldots,n) \tag{A8}$$

Substituting equation (A7) into equation (A8), yields

$$\varepsilon(3\lambda+3\rho+\mu)\sin2\theta_j-\left(1-\delta_{jn}\right)\varepsilon\left\{\frac{3}{2}\rho\sin2\left(\theta_j-\theta_{j+1}\right)\left[\frac{3}{2}\left(\cos^2\theta_j+\cos^2\theta_{j+1}\right)-1\right]\right.$$
$$\left.+\frac{3}{2}\left[\lambda+\frac{3}{2}\rho\cos^2\left(\theta_j-\theta_{j+1}\right)-\frac{1}{2}\rho\right]\sin2\theta_j+\mu\cos\theta_{j+1}\sin\left(2\theta_j-\theta_{j+1}\right)+\frac{3}{2}\nu\sin2\left(\theta_j-\theta_{j+1}\right)\right\}-\left(1-\delta_{j1}\right)$$
$$\times\varepsilon\left\{\frac{3}{2}\rho\sin2\left(\theta_j-\theta_{j-1}\right)\left[\frac{3}{2}\left(\cos^2\theta_j+\cos^2\theta_{j-1}\right)-1\right]+\frac{3}{2}\left[\lambda+\frac{3}{2}\rho\cos^2\left(\theta_j-\theta_{j-1}\right)-\frac{1}{2}\rho\right]\sin2\theta_j\right.$$
$$\left.+\mu\cos\theta_{j-1}\sin\left(2\theta_j-\theta_{j-1}\right)+\frac{3}{2}\nu\sin2\left(\theta_j-\theta_{j-1}\right)\right\}-\eta_a\left(H_x\sin\theta_j+H_z\cos\theta_j\right)\left(H_x\cos\theta_j-H_z\sin\theta_j\right)=0$$
$$(j=1,2,\ldots,n) \tag{A9}$$

A.2 Three kinds of basic Fréedericksz transition

A.2.1 *The homeotropic-to-planar alignment transition*

The two interfaces of the slab are taken to be substrates, with infinitely strong homeotropic anchoring, i.e. there are equations $\theta_l=0$ and $\theta_n=0$. So equation (A9) degenerates to $n-2$ equations. Supposing the external magnetic field $\boldsymbol{H}$ applied to the NLC medium is parallel to the x-axis (i.e. $H_x=H$, $H_z=0$) and θ_j is small enough near the threshold magnetic fields, then

$$-\varepsilon(6\rho+3\nu+\mu)\left(\theta_{j-1}-2\theta_j+\theta_{j+1}\right)+\eta_aH^2\theta_j=0. \tag{A10}$$

If the two sides of equation (A10) are divided by a^3 (a is the lattice constant), we obtain

$$\frac{-\varepsilon(6\rho+3\nu+\mu)}{a}\frac{\theta_{j-1}-2\theta_j+\theta_{j+1}}{a^2}+\frac{\eta_a}{a^3}H^2\theta_j=0. \quad \text{(A11)}$$

Furthermore, one notes that $(\theta_{j-1}-2\theta_j+\theta_{j+1})/a^2$ corresponds to the difference expression of $d^2\theta/dz^2$. So equation (A11) changes to the continuous equation

$$\frac{-\varepsilon(6\rho+3\nu+\mu)}{a}\frac{d^2\theta}{dz^2}+\frac{\eta_a}{a^3}H^2\theta=0. \quad \text{(A12)}$$

Setting

$$\chi_a=\frac{\eta_a}{a^3} \text{ and } K_3=\frac{-\varepsilon(6\rho+3\nu+\mu)}{a}$$

we can obtain an equation corresponding with continuous theory. Using the same procedure as in continuous theory [26], equation (A12) can give the threshold magnetic fields

$$H_C^{(3)}=\frac{\pi}{d}\sqrt{\frac{K_3}{\chi_a}} \quad \text{(A13)}$$

where d is the thickness of the NLC slab, i.e. the thickness of the NLC cell. We also note that χ_a is the magnetic anisotropy of NLC medium if perfect nematic order is assumed.

A.2.2 *The planar-to-homeotropic alignment transition*

We choose two substrates of the slab with infinitely strong planer anchoring which favours planer alignment, i.e. the polar angles of $j=1$ and $j=n$ satisfy $\theta_1=\pi/2$ and $\theta_n=\pi/2$. Equation (A9) can be degenerated to $n-2$ equations as above. Further, we assume the external magnetic field $\boldsymbol{H}$ is parallel to the z-axis (i.e. $H_x=0$, $H_z=H$). We can set $\theta_j=(\pi/2)-\alpha_j$ in order to yield the threshold magnetic fields of the Fréedericksz transition by linear analysis. If α_j is small enough, equation (A9) gives

$$\varepsilon(3\rho-3\nu-\mu)\left(\alpha_{j-1}-2\alpha_j+\alpha_{j+1}\right)+\eta_a H^2\alpha_j=0. \quad \text{(A14)}$$

According to the analysis as above, we obtain the equations

$$\frac{\varepsilon(3\rho-3\nu-\mu)}{a}\frac{\alpha_{j-1}-2\alpha_j+\alpha_{j+1}}{a^2}+\frac{\eta_a}{a^3}H^2\alpha=0 \quad \text{(A15)}$$

$$\frac{\varepsilon(3\rho-3\nu-\mu)}{a}\frac{d^2\alpha}{dz^2}+\frac{\eta_a}{a^3}H^2\alpha=0 \quad \text{(A16)}$$

$$H_C^{(1)}=\frac{\pi}{d}\sqrt{\frac{K_1}{\chi_\alpha}} \quad \text{(A17)}$$

where

$$\chi_a=\eta_a/a^3, \quad K_1=\frac{\varepsilon(3\rho-3\nu-\mu)}{a}.$$

A.2.3 *The simple twisted transition*

We suppose that the NLC molecular layer is parallel to the $x-z$ plane as in the above discussion. We also assume that the direction of molecules changes in the $x-y$ plane and that the angle between the molecular long axis and the x-axis is ϕ. When the molecule i is in the jth layer, $\boldsymbol{u}_i=(\cos\phi_j, \sin\phi_j, 0)$. The magnetic field is in the $x-y$ plane, i.e. $\boldsymbol{H}=(H_x, H_y, 0)$. Using the same procedure that yielded equation (A9), we obtain

$$\begin{aligned}&-\frac{3}{2}\varepsilon(\nu-\rho)\left\{\left(1-\delta_{jn}\right)\sin 2\left(\phi_j-\phi_{j+1}\right)\right.\\&\left.+\left(1-\delta_{j1}\right)\sin 2\left(\phi_j-\phi_{j-1}\right)\right\}\\&-\eta_a\left(H_x\cos\phi_j+H_y\sin\phi_j\right)\left(-H_x\sin\phi_j+H_y\cos\phi_j\right)=0\\&\quad(j=1,2,\ldots,n). \quad \text{(A18)}\end{aligned}$$

In order to study the Fréedericksz transition of twist deformation, we impose infinitely strong anchoring on the x-axis, i.e. $\phi_1=\phi_n=0$. The external magnetic fields are parallel to the y-axis, i.e. $H_x=0, H_y=H$. Assuming ϕ_j is small enough, we have

$$-3\varepsilon(\nu-\rho)\left(\phi_{j-1}-2\phi_j+\phi_{j+1}\right)+\eta_a H^2\phi_j=0. \quad \text{(A19)}$$

As above, we obtain the equations

$$\frac{-3\varepsilon(\nu-\rho)}{a}\frac{\phi_{j-1}-2\phi_j+\phi_{j+1}}{a^2}+\frac{\eta_a}{a^3}H^2\phi=0 \quad \text{(A20)}$$

$$\frac{-3\varepsilon(\nu-\rho)}{a}\frac{d^2\phi}{dz^2}+\frac{\eta_a}{a^3}H^2\phi=0 \quad \text{(A21)}$$

$$H_C^{(2)}=\frac{\pi}{d}\sqrt{\frac{K_2}{\chi_a}} \quad \text{(A22)}$$

Here

$$\chi_a = \eta_a/a^3, \quad K_2 = \frac{-3\varepsilon(\nu-\rho)}{a}.$$

A.2.4 *Relations between the potential parameters and the elastic constants*

Using the relationship between the potential parameters and the elastic constants, i.e. $K_1 = (\varepsilon(3\rho - 3\nu - \mu))/a$, $K_2 = (-3\varepsilon(\nu-\rho))/a$, and $K_3 = (-\varepsilon(6\rho + 3\nu + \mu))/a$, we can obtain the potential parameters denoted by the elastic constants

$$\mu = 3\Lambda(K_2 - K_1), \tag{23a}$$

$$\nu = \frac{1}{3}\Lambda(K_1 - 3K_2 - K_3), \tag{23b}$$

$$\rho = \frac{1}{3}\Lambda(K_1 - K_3). \tag{23c}$$

Here $\Lambda = a/3\varepsilon$, which has the dimensions of length. This is consistent with equations (3b), (3c) and (3d) for M I. From the above, we cannot obtain the corresponding relation for λ. However, from [17], the terms $\lambda[P_2((a_i)) + P_2(a_k)]$ in the pair potentials cancel out identically when in three-dimensional periodic boundary conditions, i.e. the value of λ does not influence the description of the NLC bulk properties. So our model, in fact, is consistent with M I in three-dimensional periodic boundary conditions.

A.3 The director in the slab at the free surfaces

When there are no external magnetic fields and no external substrate anchoring, one can demonstrate that

$$\theta_{j-1} = \theta_j = \theta_{j+1} = \theta \tag{A24}$$

is the solution to equation (A9) for $j = 2,3,\ldots,n-1$. So the two equations for $j=1$ and for $j=n$ reduce to

$$(3\lambda + 3\rho + \mu)\sin 2\theta = 0. \tag{A25}$$

Substituting equations (A24) and (A25) into equation (A7) (external magnetic fields and external substrate anchoring are cancelled out), we find that

$$F = \sigma\varepsilon\left[(n-2)\left(\frac{2}{3}\mu + 3\nu\right) + (3\lambda + 3\rho + \mu)\sin^2\theta + \left(5\nu + \frac{4}{9}\mu\right) - 2(\lambda + \rho)\right] \tag{A26}$$

M I gives $3\lambda + 3\rho + \mu = 0$ and the director in the slab is isotropic, the same result as given in the Labwohl–Lasher model.

M II satisfies $3\lambda + 3\rho + \mu = \Lambda(K_1 - K_3)$. If $3\lambda + 3\rho + \mu > 0$ (i.e. $K_1 > K_3$), equation (A26) gives $\theta = 0$ (homeotropic alignment to free surfaces) so that the total energy of the sample is lowest. If $3\lambda + 3\rho + \mu < 0$ (i.e. $K_1 < K_3$), $\theta = \pi/2$ (planer alignment with the free surfaces). For example, the molecules of PAA which satisfies $3\lambda + 3\rho + \mu < 0$ align along the free surface. It is consistent with the experimental observation [9].

By our model, $3\lambda + 3\rho + \mu = 3\lambda - \Lambda(2K_1 - 3K_2 + K_3)$. We set $3\lambda + 3\rho + \mu = \zeta$, where ζ is a constant. When ζ is positive, the free interfaces favour homeotropic alignment ($\theta = 0$); When ζ is negative, the free interfaces favor planer alignment ($\theta = \pi/2$); when ζ is zero (i.e. MI), the free interfaces cannot produce any orienting effects. So we can introduce a modification of λ for MI, i.e. $\lambda + c$ instead of λ, to describe the behaviour of interfaces. The relation between ζ and c is $\zeta = 3c$.

References

[1] W. Maier and A. Saupe, Z. Naturforsch. **14a,** 882 (1959).
[2] W. Maier and A. Saupe, Z. Naturforsch. **15a,** 287 (1960).
[3] P. A. Lebwohl and G. Lasher, Phys Rev. **A6,** 426 (1972).
[4] T. Gruhn and S. Hess, Z. Naturforsch. **51a,** 1 (1996).
[5] S. Romano, Int. J. Mod. Phys. **B12,** 2305 (1998).
[6] S. Romano, Phys. Lett. **A310,** 465 (2003).
[7] G. P. Crawford and S. Žumer (eds), *Liquid Crystals in Complex Geometries: Formed by Polymer and Porous Networks* (Taylor and Francis, London, 1996).
[8] N. V. Priezjev, G. Skačej, R. A. Pelcovits, and S. Žumer, Phys. Rev. E **68,** 041709 (2003).
[9] M. A. Bouchiat and D. Langevin-Cruchin, Phys. Lett. **34A,** 331 (1971).
[10] P. Chiarelli, S. Faetti, and L. Fronzoni, J. Phys. (Paris) **44,** 1061 (1983).
[11] L. M. Blinov, A. Yu. Kabayenkov, and A. A. Sonin, Liq. Cryst. **5,** 654 (1989).
[12] L. R. Evangelista and S. Ponti, Phys. Lett. A **197,** 55 (1995).
[13] J. G. Gay and B. J. Berne, J. Chem. Phys. **74,** 3316 (1981).
[14] E. Martin del Rio and E. de Miguel, Phys. Rev. E **55,** 2916 (1997).
[15] A. P. J. Emerson, S. Faetti, and C. Zannoni, Chem. Phys. Lett. **271,** 241 (1997).
[16] S. J. Mills, C. M. Care, M. P. Neal, and D. J. Cleaver, Phys. Rev. E **58,** 3284 (1998).
[17] A. Kilian, Liq. Cryst. **14,** 1189 (1993).
[18] Y. J. Zhang, Z. D. Zhang, J. P. Cui, and H. P. Wei, Chinese J. Liq. Cryst. Displays **21,** 201, in Chinese (2006).
[19] G. R. Luckhurst and S. Romano, Liq. Cryst. **26,** 871 (1999).
[20] Z. D. Zhang and Y. J. Zhang, Acta Phys. Sin. **53,** 2670, in Chinese (2004).

[21] Z. D. Zhang, H. Yu, and L. Li, Chin. Phys. **10,** 645 (2001).
[22] P. G. De Gennes and J. Prost (eds), *The Physics of Liquid Crystals*, 2nd edn (Oxford University Press, Oxford, 1995), p. 103.
[23] D. A. Dunmar, A. Fukuda, and G. R. Luckhurst, *Physical Properties of Liquid Crystals: Nematics* (Institution of Electrical Engineers, London, 2001), p. 588.
[24] N. Metropolis, A. W. Rosenbluth, M. N. Rosenbluth, *et al*., J. Chem. Phys. **21,** 1087 (1953).
[25] Z. D. Zhang, D. X. Zhang, and Y. B. Sun, Chin. Phys. Lett. **17,** 749 (2000).
[26] R. Barberi and G. Barbero, in *Physics of Liquid Crystalline Materials*, edited by I. C. Khoo and F. Simoni (Gorden and Breach Science Publishers, Philadelphia, 1991), p. 215.